Intermolecular Hydroacylation: High Activity Rhodium Catalysts Containing Small-Bite-Angle Diphosphine Ligands

Adrian B. Chaplin,[†] Joel F. Hooper,[‡] Andrew S. Weller,*[,†] and Michael C. Willis*[,‡]

[†]Department of Chemistry, Inorganic Chemistry Laboratories, University of Oxford, South Parks Road, Oxford OX1 3QR, U.K.

[‡]Department of Chemistry, University of Oxford Chemistry Research Laboratory, Mansfield Road, Oxford OX1 3TA, U.K.

Ⓢ *Supporting Information*

ABSTRACT: Readily prepared and bench-stable rhodium complexes containing methylene bridged diphosphine ligands, viz. $[Rh(C_6H_5F)(R_2PCH_2PR'_2)][BAr^F_4]$ (R, R' = ^tBu or Cy; Ar^F = C_6H_3-3,5-$(CF_3)_2$), are shown to be practical and very efficient precatalysts for the intermolecular hydroacylation of a wide variety of unactivated alkenes and alkynes with β-S-substituted aldehydes. Intermediate acyl hydride complexes $[Rh(^tBu_2PCH_2-P^tBu_2)H\{\kappa^2(S,C)\text{-}SMe(C_6H_4CO)\}(L)]^+$ (L = acetone, MeCN, $[NCCH_2BF_3]^-$) and the decarbonylation product $[Rh-(^tBu_2PCH_2P^tBu_2)(CO)(SMePh)]^+$ have been characterized in solution and by X-ray crystallography from stoichiometric reactions employing 2-(methylthio)benzaldehdye. Analogous complexes with the phosphine 2-(diphenylphosphino)-benzaldehyde are also reported. Studies indicate that through judicious choice of solvent and catalyst/substrate concentration, both decarbonylation and productive hydroacylation can be tuned to such an extent that very low catalyst loadings (0.1 mol %) and turnover frequencies of greater than 300 h^{-1} can be achieved. The mechanism of catalysis has been further probed by KIE and deuterium labeling experiments. Combined with the stoichiometric studies, a mechanism is proposed in which both oxidative addition of the aldehyde to give an acyl hydride and insertion of the hydride into the alkene are reversible, with the latter occurring to give both linear and branched alkyl intermediates, although reductive elimination for the linear isomer is suggested to have a considerably lower barrier.
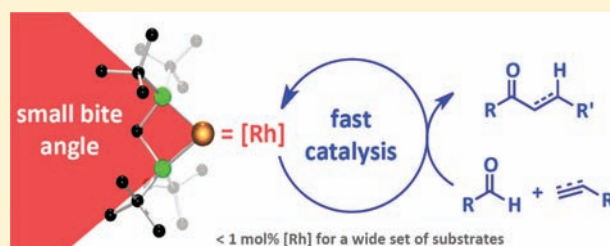
■ INTRODUCTION

The hydroacylation reaction is a potentially powerful transformation in organic and materials synthesis, that allows for the 100% atom-efficient production of ketones from the combination of an alkene or alkyne with an aldehyde by sequential C−H activation and C−C bond formation (eq 1).[1−4] These

$$R\overset{O}{\underset{H}{\diagdown}} + \;\equiv\!\!-R' \;\xrightarrow{[cat.]}\; R\overset{O}{\diagdown}\!\!-R' \qquad (1)$$
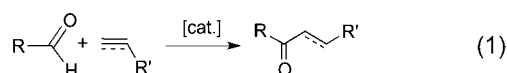
processes are at present best catalyzed by cationic rhodium−diphosphine complexes, as first reported by Bosnich, e.g. $[Rh(dppe)]_2^{2+}$.[5,6] These are complemented by $[MCp(\eta^2\text{-}H_2C=CHSiMe_3)_2][BAr^F_4]$ (M = Co, Rh; Ar^F = C_6H_3-3,5-$(CF_3)_2$) catalysts developed by Brookhart.[7,8] The accepted mechanism for this reaction with a diphosphine catalyst (Scheme 1)[1,4−6,8−12] involves aldehyde oxidative addition to give an acyl hydride intermediate (**A**) followed by alkene coordination and hydride insertion (rather than acyl migration) to give complex **C**, at which point linear/branched selectivity can also arise.[13,14] Reductive elimination of the ketone product completes the cycle and is generally accepted to be turnover limiting for alkene hydroacylation.[6−8,10,11] Extension of this methodology to carbonyl hydroacylation is also known.[12,15−17] Recently, ruthenium hydrides have also been shown to promote

Scheme 1. Mechanism for Linear-Selective Alkene Hydroacylation Using Rh-Diphosphine Catalysts
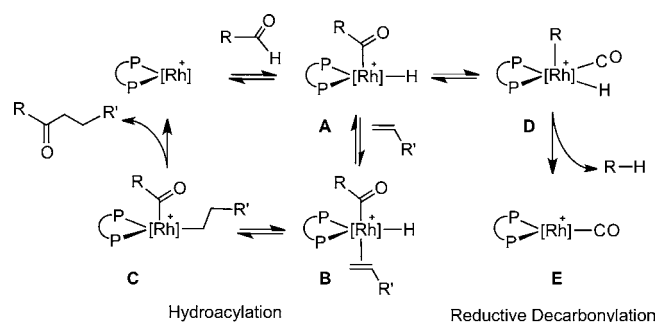
hydroacylation, although the mechanism is different from that proposed for rhodium catalysts.[18,19]

The Achilles heel of this process is the irreversible reductive decarbonylation from the acyl hydride (**A** to **E** via **D**), that generates R−H (R = alkyl or aryl) and a considerably less active metal−carbonyl. The carbonyl deinsertion step in this process requires a vacant coordination site *cis* to the acyl.[20] For intramolecular hydroacylation, for example using 4-pentenals,[5,21,22]

decarbonylation is attenuated by chelate-assisted olefin coordination. For intermolecular hydroacylation, substrate-derived chelation-assisted strategies have also been developed to address decarbonylation,[4,23−27] in which carbonyl deinsertion is disfavored due to ring strain. For example, we have developed the use of β-S-substituted aldehydes to deliver productive hydroacylation catalysis using dppe-derived Rh(I) catalysts.[28−34] A complementary, catalyst-centered, approach is the use of the hemilabile diphosphine ligand, DPEphos, that reversibly binds to the *cis*-vacant site while also allowing access by the olefin.[10,35] An alternative methodology involves the use of Cp*−Rh(I) derived catalysts. In these systems reversible carbonyl deinsertion occurs (and is in fact the resting state in catalysis), but reductive elimination is unfavorable in the co-ordinatively saturated alkyl-hydrido-carbonyl intermediate.[7,8] These approaches, designed to attenuate the deleterious reductive decarbonylation, still only deliver intermolecular hydroacylation catalysts that operate at relatively high loadings of 5−10 mol %.[4,36]

A more refined approach to the development of catalysts that operate at low loadings (ideally less than 1 mol %), and for a wide range of substrates, would be to selectively increase the rate of ketone reductive elimination—the step that is accepted to be rate-limiting for alkene hydroacylation. This could be achieved sterically, by the use of bulky diphosphine ligands, or electronically, by variation of the ligand bite-angle or inclusion of electron-withdrawing substituents.[8,37−40] However, within the context of olefin hydroacylation with β-S-substituted aldehydes, recent results using wide-bite-angle ligands such as $Ph_2P(CH_2)_5PPh_2$ or sterically bulky ligands such as $(o\text{-}^iPrC_6H_4)_2P(CH_2)_2P(o\text{-}^iPrC_6H_4)_2$ demonstrate that they are not suitable for delivering linear-selective intermolecular alkene hydroacylation. For example, while the overall rate of reaction can be increased significantly with increasing bite-angle using $Ph_2P(CH_2)_nPPh_2$ (n = 2−5), there are selectivity changes between aldehyde versus alkene hydroacylation.[13] Branched-selective catalysis is favored over linear-selective when using the sterically bulky ligand $(o\text{-}^iPrC_6H_4)_2P(CH_2)_2P(o\text{-}^iPrC_6H_4)_2$ in alkyne hydroacylation.[14] Use of the wide-bite-angle POP ligand Xantphos results in irreversible oxygen coordination at the rhodium center, giving an inactive acyl hydride.[13]

Mindful of these results, we turned to small-bite-angle electron-rich ligands, $R_2P(CH_2)PR'_2$, developed by Hoffmann R, R′ = ^tBu or Cy[41−43] (Scheme 2), in an effort to deliver both

Scheme 2. Small-Bite-Angle Phosphine Ligands Used in This Study
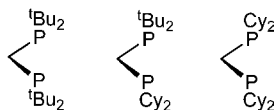
fast and selective catalysis. These ligands, with their compressed P−M−P bite-angles, promote *cis*-geometries and low-coordinate monomeric T-shaped Rh(I) RhL_2X intermediates.[41,44] As low-coordinate intermediates are also necessary for reductive elimination, especially in systems derived from 6-coordinate d^6 metal complexes,[45,46] we reasoned that similar complexes might be accessible in the Rh(III) intermediates such as **C** using these small-bite-angle ligands. Indeed, Werner has commented that Rh(III) fragments of the type $[Rh(^iPr_2PCH_2P^iPr_2)]^+$ promote reductive elimination reactions more readily than nonchelate

systems due to ring strain imposed by the chelate ring.[47] Reductive elimination of H_2 from $[H_2Rh(PP)_2]^+$ complexes (PP = chelating diphosphine) has also been shown to be heavily influenced by the natural bite-angle of the diphosphines. Small-bite-angle diphosphines favor Rh(I) complexes (i.e., reductive elimination) $[Rh(PP)_2]^+$ while larger bite-angle diphosphines favor Rh(III) complexes $[H_2Rh(PP)_2]^+$.[48,49]

We were also encouraged by the report by Fink that reductive elimination of ethane from $\{Cy_2PCH_2PCy_2\}PdMe_2$ was rapid, while complexes with longer chain chelates only did so slowly.[50] It was suggested that Pd−P dissociation of one of the phosphine arms in this d^8 system might lead to rapid reductive elimination via a T-shaped intermediate, although in other related d^8 systems such intermediates have been discounted on the basis of computational and NMR spectroscopy studies.[51] Small-bite-angle ligands based upon $R_2PCH_2PR_2$ and $R_2PNR'PR_2$ have also been success-fully used in ethene oligomerizations mediated by chromium catalysts, in which subtle variation of ligand electronics and sterics leads to changes in selectivity.[52] Although the mechanism is very complex,[53] controlling the rate of reductive elimination of the final product (e.g., 1-hexene) is implicit.

Here we report the development of new rhodium catalysts, containing the small-bite-angle diphosphine ligands $R_2PCH_2PR'_2$ (R, R′ = ^tBu, Cy) for the intermolecular hydroacylation of a wide variety of unactivated alkenes and alkynes with β-S-substituted aldehydes. Mechanistic studies indicate that, through judicious choice of solvent and catalyst/substrate concentration, both the decarbonylation and the productive reaction can be tuned to such an extent that very low catalyst loadings (0.1 mol %) and turnover frequencies of greater than 300 h^{-1} can now be achieved. Moreover, these catalyst systems are readily prepared and bench-stable.

■ RESULTS AND DISCUSSION

Synthesis of the Diphosphine Catalyst Precursors. On the basis of previous work on the stabilization of low coordinate bis-phosphine rhodium(I) fragments using the weakly coordi-nating fluorobenzene ligand,[54−56] we targeted the synthesis of $[Rh(C_6H_5F)(R_2PCH_2PR'_2)][BAr^F_4]$ (**1a**, R = R′ = Cy; **1b**, R = Cy, R′ = ^tBu; **1c**, R = R′ = ^tBu) as well-defined catalyst precursors for these studies. These complexes were readily prepared using a simple one-pot procedure involving addition of the diphosphine ligands to $[Rh(COD)_2][BAr^F_4]$ (COD = 1,5-cyclooctadiene) in C_6H_5F solution and subsequent hydro-genation (Scheme 3). Precipitation with pentane afforded **1a−c** as yellow microcrystalline solids with high isolated yields (>70%). These three new complexes were fully characterized by NMR spectroscopy, ESI-MS, and elemental microanalysis. An important practical observation for these systems is that they are air-stable and are able to be stored in vials on the bench.

The room-temperature ^1H NMR spectra of **1a−c** in CD_2Cl_2 solution show characteristic, total integral 5H, upfield shifted resonances for η^6-coordinated fluorobenzene ligands (δ 6.0−6.8, cf. δ 7.0−7.4 for free ligand). This coordination was also demonstrated by ^{13}C and ^{19}F NMR spectroscopy, with the later revealing coordinated fluorobenzene resonances at ca. δ −123 (cf. δ −113.9 for free ligand). Single ^{31}P environments were observed for **1a** (δ −8.6) and **1c** (δ 14.9), that show coupling to ^{103}Rh ($^1J(RhP)$ = 170 and 176 Hz, respectively). For **1b** the different ^{31}P environments are observed at δ −12.7 and 17.9 as

Scheme 3. Preparation of Diphosphine Catalyst Precursors 1a–c

1a, R = R' = Cy; 1b, R = Cy, R' = ᵗBu; 1c, R = R' = ᵗBu   3
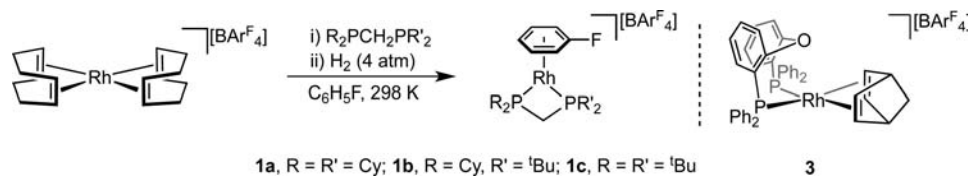
doublets of doublets, with a $^2J(PP)$ coupling constant of 83 Hz and $^1J(RhP)$ coupling constants of ca. 173 Hz. ESI-MS, which shows strong molecular-ion peaks with retention of fluorobenzene, and microanalysis confirm the empirical formulas. Taken together, these data fully support the structures shown for **1a–c**.

The solid-state structures of **1a–c** have also been determined by single crystal X-ray diffraction. That of **1c** is shown in Figure 1,
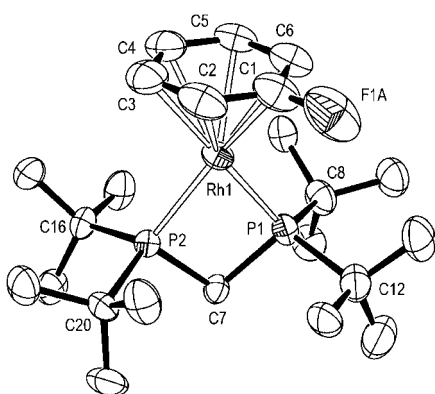

Figure 1. Solid-state structure of **1c**; displacement ellipsoids depicted at the 50% probability level. One of the two independent molecules in the asymmetric unit is shown. Hydrogen atoms, anion, and disordered components (C_6H_5F ligand, two ᵗBu groups) omitted for clarity. Key bond lengths (Å) and angles (deg): Rh1–P1, 2.263(2); Rh1–P2, 2.2711(15); Rh1–C, 2.298(4)–2.341(4); P1–Rh1–P2, 74.57(5); P1–C7–P2, 95.7(3); Rh2–P11, 2.2591(15); Rh2–P12, 2.2546(15); Rh2–C, 2.22(3)–2.36(4); P11–Rh2–P12, 74.44(5); P11–C107–P12, 95.1(3).

with the others given in the Supporting Information. A closely related compound to **1c** featuring the more coordinating benzene ligand has previously been reported, $[Rh(C_6H_6)-(^tBu_2PCH_2P^tBu_2)][BF_4]$.[57] These four structures show comparable geometries and, correspondingly, similar structural metrics. Although in the structures of **1a–c**, the fluorobenzene ligands are disordered, all clearly demonstrate the η^6-coordination of the arene to the metal center with Rh–C distances, e.g. 2.22(3)–2.36(4) Å in **1c**, being similar to those in other fluorobenzene Rh(I) complexes, viz. $[Rh(Ph_2P(CH_2)_2PPh_2)(C_6H_5F)][BAr^F_4]$ (2.292(4)–2.377(4) Å)[56] and $[Rh(P^iBu_3)_2(C_6H_5F)][BAr^F_4]$ (2.299(9)–2.411(7) Å).[55] The diphosphine bite-angles in **1a** and **1b** are the same within error, viz. 72.78(3)° and 72.86(3)°, respectively, although they are slightly smaller in comparison to those for **1c** [74.57(5)°, 74.44(5)° (Z' = 2)] and $[Rh(C_6H_6)-(^tBu_2PCH_2P^tBu_2)][BF_4]$ (74.29°).[57]

Catalyst Evaluation—Intermolecular Hydroacylation. With the PCP-catalysts **1a–c** in hand, we evaluated their activity in three simple, but relatively challenging, intermolecular reactions: the hydroacylation of 1-hexene, norbornadiene, and 1-octyne, all with 2-(methylthio)benzaldehdye (**2**). Catalyst loadings were 10 mol %, and dichloroethane was
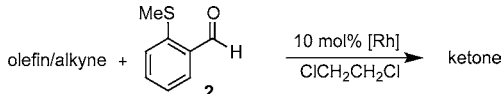
used as the solvent. The DPEphos-ligated complex [Rh-(DPEphos)(nbd)][BAr^F_4] (**3**; nbd = norbornadiene), which has previously been shown to catalyze the hydroacylation of 1-hexene or 1-octyne with **2**,[10] was used as a benchmark for these reactions (Table 1). Catalyst **3** requires pretreatment with H_2 to produce the active species, whereas **1a–1c** were used directly.

The results in Table 1 demonstrate that **1a–c** significantly outperform **3** and are the most efficient catalysts reported to date for these substrates. Within this manifold, certain catalysts appear to perform better with different substrates: **1c** is slightly more effective for promoting the hydroacylation of 1-hexene than **1a** (94% versus 86%, respectively), while, for the hydroacylation of 1-octyne, **1a** is better than **1c** (95% versus 90%). The precise reason(s) for these differences is currently unresolved, but given the similar P–Rh–P bite-angles for these catalysts, they most likely result from the steric profile of the ligands. Consistent with this idea, the mixed phosphine catalyst **1b** is intermediate in both rate and conversion between **1a** and **1c** for these hydroacylation reactions (Table 1). Despite the much slower rate for the hydroacylation of nbd, compared to 1-hexene, high conversions are still achieved using the PCP-catalysts (i.e., 96% for **1a**). The slower rate is attributed to the intermediate (reversible) formation of Rh(I) nbd-adducts, i.e. $[Rh(nbd)(R_2PCH_2PR'_2)][BAr^F_4]$. For **3**, we suggest that nbd is too strongly bound to allow hydroacylation to occur.

A time course plot of the hydroacylation of 1-hexane using **1a**, **1c**, and **3** (conversions determined using HPLC) is shown in Figure 2. These data show that both PCP-catalysts have considerably faster initial rates than **3**, but they appear to deactivate (presumably via reductive decarbonylation, vide infra) over time. We discount significant product inhibition is occurring, as addition of 50 mol % of ((o-methylthio)phenyl)-nonan-1-one (the ketone product of octene hydroacylation with **2**) to the initial catalytic mixture resulted in only a small reduction in overall conversion when using **1c**.

Encouraged by the very fast hydroacylation rates observed using the small-bite-angle diphosphine ligands, we next investigated the organometallic chemistry and the resulting catalytic pathways in greater detail. We selected the ᵗBu substituted complex **1c**, as this provided a good combination of a fast rate of catalysis and ease of solution ^1H and ^{31}P NMR characterization.

Model Complexes Using 2-(Diphenylphosphino)-benzaldehyde. The reaction of **1c** with the phosphine tethered aldehyde 2-(diphenylphosphino)benzaldehyde was first investigated. This aldehdye has previously been employed in hydroacylation reactions in combination with rhodium catalysts,[58,59] but the strongly coordinating nature of the phosphine tether necessitates the use of forcing reaction conditions to promote turnover. However, this stability lends itself to the ability to characterize stable model complexes. Addition of 2-(diphenylphosphino)benzaldehyde to **1c** in d_6-acetone at room temperature resulted in rapid cyclometalation[60]

Table 1. Screening of 1a−c and 3 as Alkene and Alkyne Hydroacylation Catalysts[a]

Substrate	Product	Catalyst	Time (hrs)	Yield (%)[b]
1-hexene		1a	1	86
		1b	0.58	91
		1c	0.25	94
		3[c]	36	71
nbd		1a	22	96
		1b	36	94
		1c	72	68
		3	72	0
1-octyne[d]		1a	0.25	95
		1b	1.25	95
		1c	6	90
		3[c]	72	11[e]

[a]Conditions: aldehyde (1.0 equiv, 0.075 M), alkene, or alkyne (1.5 equiv), 10 mol % catalyst, ClCH$_2$CH$_2$Cl, 353 K. [b]Isolated yield. [c]Catalyst was pretreated with hydrogen. [d]298 K. [e]Linear: branched ratio 10:1; at 353 K, 93% yield after 2 h as a 2:1 L/B ratio.
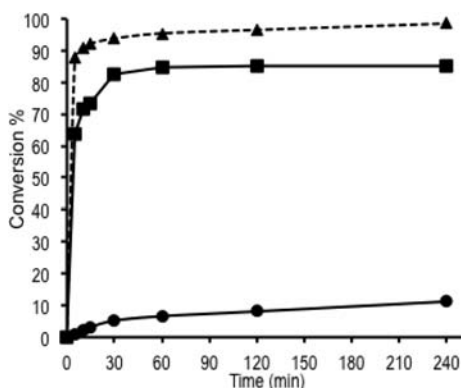

Figure 2. Time course plot for the hydroacylation of 1-hexene (1.5 equiv) with **2** (1.0 equiv, 0.075 M) catalyzed by **1c** (▲), **1a** (■), or **3** (●). Conditions: 10 mol % catalyst, ClCH$_2$CH$_2$Cl, 353 K.

(less than 5 min) and formation of the acyl hydride complex [Rh(^{t}Bu$_2$PCH$_2$P^{t}Bu$_2$)H{κ^2(P,C)-PPh$_2$(C$_6$H$_4$CO)}(OCMe$_2$)]-[BAr$^F_4$] (**4**) quantitatively by NMR spectroscopy (Scheme 4). The formation of **4** is readily apparent from NMR spectroscopy (Supporting Information). In particular, a relatively sharp high field doublet of apparent quartets at δ −19.4 is observed in the ^{1}H NMR spectrum, while the ^{31}P{^{1}H} NMR spectrum (250 K) shows three well-resolved doublet of doublet of doublets (AHPX spin system) at δ 57.9, 30.8, and 9.8. All the phosphine environments show coupling to ^{103}Rh, although the magnitude of coupling to P$_B$ is significantly reduced in comparison (^{1}J(RhP) = 47 Hz, cf. 126 and 113 Hz), consistent with its coordination opposite a high $trans$-influence acyl ligand. Similar magnitudes for ^{103}Rh coupling have been observed in other $trans$ acyl Rh-chelate phosphine complexes,[10,14,47,61] while Rh-acyl

complexes with the small-bite-angle ligands R$_2$PCH$_2$PR$_2$ have been reported previously.[47,61] Together these NMR data indicate that the phosphine and acyl groups lie coplanar, with the hydride ligand in an axial position in a similar way to that found for [Rh{κ^2(P,P)-DPEphos}(MeSC$_6$H$_4$CO)H(MeCN)]$^+$ [10] but, interestingly, different from that in [Rh(o-^{i}PrC$_6$H$_4$)$_2$P(CH$_2$)$_2$P(o-^{i}PrC$_6$H$_4$)$_2$(MeSC$_6$H$_4$CO)H]$^+$, where the hydride is $trans$ to a phosphine and the acyl $trans$ to the vacant site.[14] We suggest the coordination sphere in **4** is completed by weak coordination of an acetone ligand $trans$ to the hydride ligand, as the hydride chemical shift of δ −19.4 does not reflect a $trans$ vacant site.[62] Complex **4** is stable in d_6-acetone solution, and no significant changes are observed by ^{1}H and ^{31}P NMR spectroscopy after 5 days in solution at 298 K. This is in contrast to the equivalent complex of aldehyde **2**, in which reductive decarbonylation occurs relatively rapidly (vide infra). The acetonitrile adduct [Rh(^{t}Bu$_2$PCH$_2$P^{t}Bu$_2$)H{κ^2(P,C)-PPh$_2$(C$_6$H$_4$CO)}(NCMe)]-[BAr$^F_4$] (**5**) can be formed on addition of excess acetonitrile to **4** (Scheme 4).[63] Addition of ethylene to **4** at room temperature resulted in the slow formation of [Rh(^{t}Bu$_2$PCH$_2$P^{t}Bu$_2$)-{κ^2(P,O)-PPh$_2$(C$_6$H$_4$COEt)}][BAr$^F_4$] (**6**) over a period of 12 h (Scheme 5). Complex **6** is the rhodium(I) adduct of the product of ethylene hydroacylation with 2-(diphenylphosphino)-benzaldehyde. This reaction has been reported previously under catalytic conditions, using [Rh(COD)Cl]$_2$ as a catalyst, with both ethene and 1-hexene, but the organometallic intermediates were not reported.[58]

These model complexes provide a firm spectroscopic footing to study those formed with the more weakly coordinating thioether functionalized aldehyde 2-(methylthio)benzaldehyde (**2**), which we now discuss.
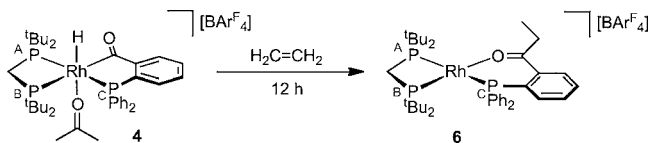
Characterization of Intermediates Using Aldehyde 2. Addition of aldehyde **2** to a CH$_2$Cl$_2$ solution of **1c** results in the initial formation of the Rh(I) aldehyde adduct

Scheme 4. Formation of Acyl Hydride Complexes 4 and 5
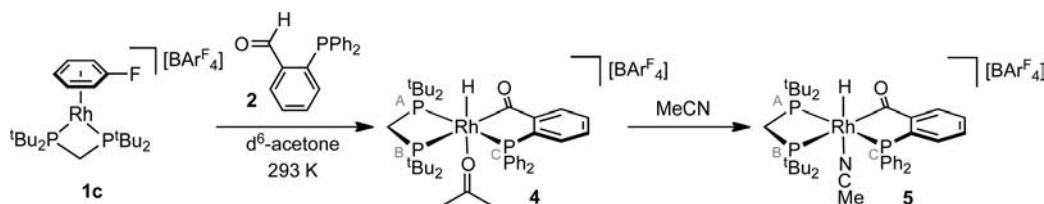
Scheme 5. Addition of Ethylene to Acyl Hydride Complex 4

$[Rh(^tBu_2PCH_2P^tBu_2)\{\kappa^2(S,O)\text{-}SMe(C_6H_4CHO)\}][BAr^F_4]$ (**7**), which proceeds to give $[Rh(^tBu_2PCH_2P^tBu_2)(CO)\text{-}(SMePh)][BAr^F_4]$ (**8**), the product of reductive decarbonylation (Scheme 6). No acyl hydride intermediate was observed. These two processes have been modeled using a two-step first-order kinetic model (Supporting Information), in which formation of **7** and **8** occur with rate constants of $(1.59 \pm 0.02) \times 10^{-4}$ s^{-1} and $(1.75 \pm 0.03) \times 10^{-4}$ s^{-1} respectively ($t_{1/2} = 1.10 \pm 0.02$ h). Compound **7** was characterized in situ, while **8** could be isolated in good yield as a microcrystalline yellow solid. NMR data for **7** and **8** are fully consistent with their formulation. In particular, both show inequivalent, mutually coupled, ^{31}P environments to a Rh(I) center. Furthermore, the ^{1}H NMR spectrum of **7** shows the coordinated aldehyde at δ 9.47 (cf. free **2** δ 10.3) and bound thioether at δ 2.63 (cf. free **2** δ 2.49). The solid-state structure of **8** has been determined (Figure 3) and is fully consistent with the solution NMR data. The bond metrics for the coordinated thioether are similar to those reported for the decarbonylation product for the same aldehyde from the DPEphos system $[Rh(\kappa^2(P,P)\text{-}DPEphos)(CO)\text{-}(SMeEt)][CB_{11}H_6I_6]$.[10] Notably, the Rh–P distances *trans* to the carbonyl are longer than that *trans* to the thioether [2.3719(7) and 2.2779(7) Å, respectively], consistent with the differing *trans* influences of these ligands. To put the characterization of **7** on a firm footing, we have also prepared the stable ketone analogue, $[Rh(^tBu_2PCH_2P^tBu_2)(\kappa^2(S,O)\text{-}MeCOC_6H_4SMe)][BAr^F_4]$ (**9**) (Scheme 6) by addition of 2-(methylthio)acetophenone to **1c**, which has very similar NMR spectroscopic data to that of **7**.

An acyl hydride intermediate was not observed in CH$_2$Cl$_2$, presumably because this putative 5-coordinate species rapidly undergoes carbonyl deinsertion and reductive elimination to form **8**, a process that would be slowed by blocking the sixth coordination site. With DPEphos (or related ligands), this is achieved by coordination of the central oxygen atom.[10,13] Such stabilization is not possible in these small-bite-angle systems. Instead, we reasoned that changing the solvent to acetone could provide stabilization for the acyl hydride intermediate. Dissolving **1c** in acetone results in an equilibrium being established between **1c** and the bis-acetone adduct
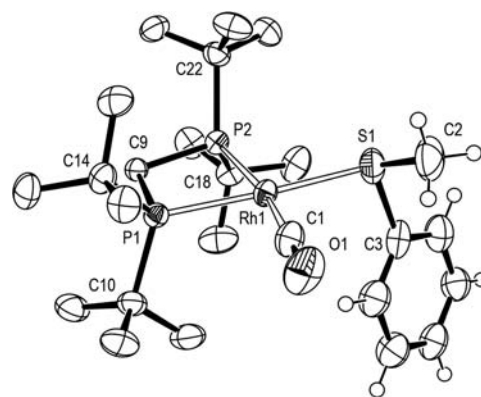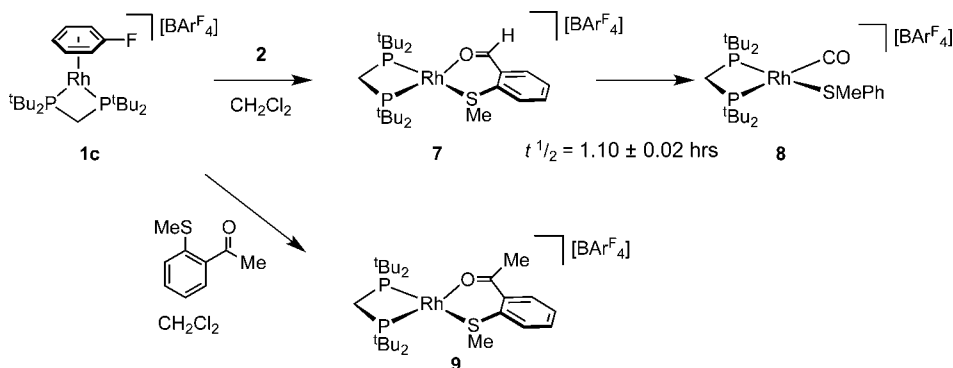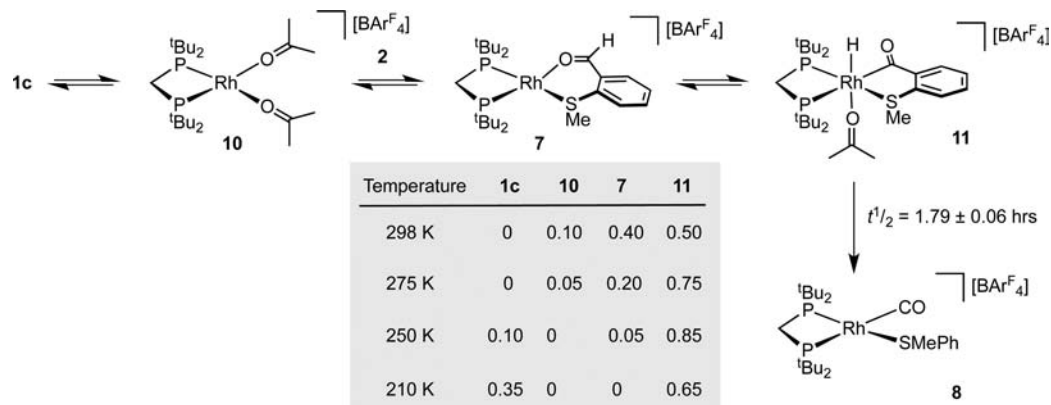

Figure 3. Solid-state structure of **8**; displacement ellipsoids depicted at the 50% probability level. Most hydrogen atoms, anion, and disordered components (Ph group) omitted for clarity. Key bond lengths (Å) and angles (deg): Rh1–P1, 2.2779(7); Rh1–P2, 2.3719(7); Rh1–C1, 1.867(3); Rh1–S1, 2.3797(8); P1–Rh1–P2, 74.36(2); P1–C9–P2, 98.23(12); P1–Rh1–C1, 94.50(10); P2–Rh1–C1, 168.69(10); C1–Rh1–S1, 96.15(10); P1–Rh1–S1, 168.79(3); P2–Rh1–S1, 95.09(3); Lsq plane (Rh1, P1, P2, S1, C1), rms deviation = 0.047.

$[Rh(^tBu_2PCH_2P^tBu_2)(OCMe_2)_2][BAr^F_4]$ (**10**) (**1c/10** = 1:6.5 at 0.015 M and 298 K). Adding 1.5 equiv of aldehyde **2** to this mixture resulted in a new equilibrium mixture containing **1c**, **10**, **7**, and the acyl hydride $[Rh(^tBu_2PCH_2P^tBu_2)H\{\kappa^2(S,C)\text{-}SMe(C_6H_4CO)\}(OCMe_2)][BAr^F_4]$ (**11**). Although the relative concentration of these species changes with temperature, demonstrating dynamic equilibrium (Scheme 7), over all temperatures **11** is the major species present. Reversible oxidative addition of aldehyde **2** has been observed previously in the $[Rh(o\text{-}^iPrC_6H_4)_2P(CH_2)_2P(o\text{-}^iPrC_6H_4)_2)]^+$ system[14] as well as in other hydroacylation systems.[6,8,12] Complex **11** was characterized in situ by NMR spectroscopy and also by comparison with the relatively stable MeCN adduct analogue (vide infra). At room temperature for **11**, broad resonances are observed for the methylene and ^{t}Bu protons as well as a hydride signal at δ −20.29 in the ^{1}H NMR spectrum. Two broadened environments are observed in the ^{31}P NMR spectrum. At 210 K these two ^{31}P environments are sharp and display very different coupling to ^{103}Rh, δ 36.2 (^1J(RhP) = 131) and 9.4 (^1J(RhP) = 57), consistent with a Rh(III) center and the different *trans*-influence of thioether over acyl, respectively. These data are similar to those for **4** and **5**. The hydride signal in the ^{1}H NMR spectrum at this temperature is also sharp and is observed at δ −20.18 as a doublet of doublet of doublets that collapses to a doublet in the ^{1}H{^{31}P} NMR spectrum. Four environments are

Scheme 6. Reactivity of 1c in CH$_2$Cl$_2$

Scheme 7. Reaction of 1c with 2 in d_6-Acetone[a]

Temperature	1c	10	7	11
298 K	0	0.10	0.40	0.50
275 K	0	0.05	0.20	0.75
250 K	0.10	0	0.05	0.85
210 K	0.35	0	0	0.65

$t^1/_2 = 1.79 \pm 0.06$ hrs

[a]Composition determined using ^{1}H and ^{31}P{^{1}H} NMR spectroscopy; error estimated to be ±5%.

Scheme 8. Reactivity of MeCN-Ligated Complexes with 2

$t^1/_2 = 38 \pm 2$ hrs
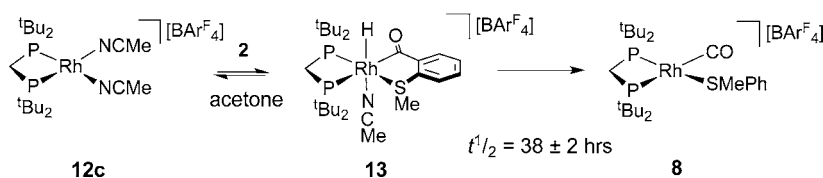
now observed for the ^{t}Bu protons and two for the methylene protons on the phosphine backbone. At low temperature, the SMe group is observed as a doublet at δ 2.66, showing coupling to ^{31}P{^{1}H} that collapses to a singlet in the ^{1}H{^{31}P} NMR spectrum.

This equilibrium mixture changes with time, reflecting the irreversible formation of the decarbonylation product **8**. The formation of **8** follows first-order reaction kinetics with a rate constant of $(1.08 \pm 0.04) \times 10^{-4}$ s^{-1} ($t_{1/2} = 1.79 \pm 0.06$ h), and the reaction proceeds to completion after 10 h. This rate is slower than that for the same reaction in CH$_2$Cl$_2$ [$t_{1/2} = (1.10 \pm 0.02$ h)]. The stabilizing role of acetone is also apparent through the observation of the acyl hydride intermediate **11** in this solvent, in contrast to CH$_2$Cl$_2$. Repeating the reaction with a 5-fold excess of **2** gave a **7/11** ratio of 1:1.30 at 298 K. Under these conditions, the formation of **8** again followed first-order reaction kinetics with the same rate within error $(0.94 \pm 0.03) \times 10^{-4}$ s^{-1} ($t_{1/2} = 2.02 \pm 0.07$ h), consistent with a first-order process from **11**, i.e. one independent of [**2**].

In an attempt to isolate the acyl hydride intermediate cleanly, we added a stronger Lewis base, MeCN, as we have previously shown[10] that MeCN can stabilize such intermediates. Addition of a five-fold excess of MeCN at 298 K to the freshly prepared acetone equilibrium mixture resulted in the immediate formation of a mixture of the bis-acetonitrile Rh(I) adduct [Rh(^{t}Bu$_2$PCH$_2$P^{t}Bu$_2$)(MeCN)$_2$][BAr$^F_4$] (**12c**) and the acyl hydride complex [Rh(^{t}Bu$_2$PCH$_2$P^{t}Bu$_2$)H{κ^2(S,C)-SMe-(C$_6$H$_4$CO)}(NCMe)][BAr$^F_4$] (**13**) in a 1:1.2 ratio (Scheme 8). To facilitate the unambiguous characterization of these species, **12c** was prepared by reaction of **1c** with MeCN. The cyclohexyl analogue [Rh(Cy$_2$PCH$_2$PCy$_2$)(MeCN)$_2$][BAr$^F_4$] (**12a**) was also prepared in the same way. Addition of **2** to isolated **12c** also resulted in equilibrium mixtures of **12c** and **13**. When 1.5 equiv of **2** was added at 298 K, the ratio of these two species was 1:3.0, whereas addition of 5 equiv of **2** gave a ratio of 1:19.0—allowing definitive characterization of **13**. The ^{1}H and

^{31}P{^{1}H} NMR spectra of **13** are similar to those of **11** and also show that bound MeCN exchanges with the bulk solvent, as only a broad resonance is observed at δ 2.0 for free and bound MeCN. As for **4** and **5**, the hydride resonance in **13** is found at a higher frequency than that in **11** (δ −15.6), reflecting the stronger binding of MeCN compared to acetone.[62] Despite the straightforward solution synthesis of **13**, attempts to this isolate this compound in the solid state were frustrated by the rapid loss of MeCN at room temperature (under vacuum or argon), leading to a mixture of products, including **7** and **8**. A single crystal was, however, able to be grown from a CH$_2$Cl$_2$/hexane solution at 5 °C and rapidly transferred into the cold stream of an X-ray diffractometer, allowing for structural characterization (Figure 4). The structural metrics reflect the differing *trans* influences of acyl over thioether, viz. Rh1−P1 2.4545(8) Å versus Rh1−P2 2.3063(8) Å. These distances are similar to those seen in the closely related Rh(III)−acyl complexes of DPEphos ligands, as is the Rh−S distance [2.3612(9) Å].[10]

Although the MeCN ligand is labile through exchange with bulk solvent, it is strongly enough bound to attenuate decarbonylation appreciably. Decarbonylation to form **8** occurs spontaneously at 298 K from equilibrium mixtures of **12c** and **13**. Following this reaction (starting with **12c/13** = 1:3.1) revealed first-order reaction kinetics for the formation of **8**, with a rate constant of $(5.1 \pm 0.3) \times 10^{-6}$ s^{-1} ($t_{1/2} = 38 \pm 2$ h). This is markedly slower in comparison to the decarbonylation reactions in acetone and CH$_2$Cl$_2$, although it is more rapid than the analogous DPEphos system, in which oxygen coordinates $[(1.2 \pm 0.1) \times 10^{-6}$ s^{-1} ($t_{1/2} = 160 \pm 12$ h)].[54] This later observation is related to the relative availability of the vacant site (O-decoordination in a chelate versus NCMe loss).

To further investigate the stabilizing effect of nitrile-based ligands against decarbonylation, we next targeted the incorporation of commercially available [NCCH$_2$BF$_3$]$^-$ anion into the metal coordination sphere, hoping to exploit additional Coulombic anion−cation interactions. This anion was originally reported
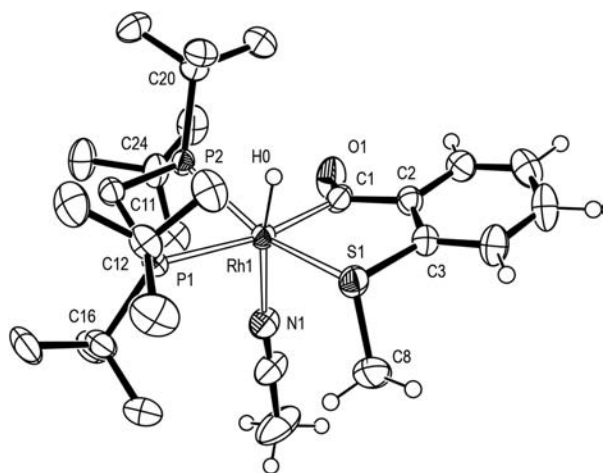
Figure 4. Solid-state structure of **13**; displacement ellipsoids depicted at the 50% probability level. Most hydrogen atoms and anion omitted for clarity. Key bond lengths (Å) and angles (deg): Rh1–P1, 2.4545(8); Rh1–P2, 2.3063(8); Rh1–C1, 2.024(3); Rh1–S1, 2.3612(9); Rh1–N1, 2.137(3); Rh1–H0, 1.46(3); P1–Rh1–P2, 74.49(3); P1–C11–P2, 101.08(15); P1–Rh1–C1, 169.07(9); P2–Rh1–C1, 95.16(9); C1–Rh1–S1, 85.15(10); P1–Rh1–S1, 103.21(3); P2–Rh1–S1, 158.78(3); H0–Rh1–N1, 171.0(13); Lsq plane (Rh1, P1, P2, S1, C1), rms deviation = 0.180.

by Molander in 2006,[64] and to our knowledge, there is no coordination chemistry reported for it. Formation of a suitable rhodium precursor incorporating this anion was achieved by addition of hydrogen to the bis-rhodium salt [Rh-(^{t}Bu$_2$PCH$_2$P^{t}Bu$_2$)(NBD)][Rh(^{t}Bu$_2$PCH$_2$P^{t}Bu$_2$)(NCCH$_2$BF$_3$)$_2$] (**14**) in the presence of excess cyclooctene. This resulted in the formation of [Rh(^{t}Bu$_2$PCH$_2$P^{t}Bu$_2$)(C$_8$H$_{14}$)(NCCH$_2$BF$_3$)] (**15**), which was isolated as an orange−yellow powder (Scheme 9). Dissolution of **15** in acetone cleanly forms the monoacetone adduct, **16**, which reacts with excess **2** to form the zwitterionic acyl hydride [Rh(^{t}Bu$_2$PCH$_2$P^{t}Bu$_2$)H{κ^2(S,C)-SMe(C$_6$H$_4$CO)}](NCCH$_2$BF$_3$)] (**17**) in quantitative yield (Scheme 10). Complex **17** was characterized by NMR spectroscopy and a single-crystal X-ray diffraction study (Figure 5). NMR data are in full accord with its formulation and are very similar to those for **11** and **13**. The structural metrics are unremarkable and show coordination of the [NCCH$_2$BF$_3$]$^-$ anion trans to the hydride. Dissolving pure **17** in acetone solvent established an equilibrium with **16**/free **2** (1:0.25, 0.015 M), further demonstrating reversible oxidative addition of aldehyde **2** in these small-bite-angle diphosphine complexes.

In the presence of a slight excess of **2** (1.5 equiv/Rh), **17** is relatively stable in solution, undergoing a slow first-order decomposition with a rate constant of $(2.7 \pm 0.3) \times 10^{-6}$ s^{-1} ($t_{1/2} = 73 \pm 9$ h), significantly slower than those observed for **11** ($t_{1/2} = 1.79 \pm 0.06$ h) and **13** ($t_{1/2} = 38 \pm 2$ h). A mixture of at least three organometallic species is observed after 10 days in solution: the major cationic species is **8** (ca. 60%) by ^{31}P NMR spectroscopy. The other species show pairs of resonances at δ

23.7 (dd, ^1J(RhP) = 124, ^2J(PP) = 43, 1P), −11.4 (dd, ^1J(RhP) = 105, ^2J(PP) = 43, 1P) (ca. 25%) and δ 20.1 (dd, ^1J(RhP) = 102, ^2J(PP) = 31, 1P), −6.0 (dd, ^1J(RhP) = 108, ^2J(PP) = 31, 1P) (ca. 15%) but remain unassigned.

Comments on Decarbonylation. Table 2 summarizes the decarbonylation data assembled from these studies. The rates of decarbonylation decrease in the order **7** (CH$_2$Cl$_2$) > **11** ≫ **13** > **17**, with no significant decarbonylation observed for **4**. As these relate to the stability of the [Rh(^{t}Bu$_2$PCH$_2$P^{t}Bu$_2$)H{κ^2(S,C)-SMe(C$_6$H$_4$CO)}]$^+$ fragment, there is a clear correlation between increased donor strength (as indicated by ^{1}H NMR shifts of the trans-hydride, where available) and the attenuation of decarbonylation, with CH$_2$Cl$_2$ providing the weakest stabilization and the anionic nitrile [NCCH$_2$BF$_3$]$^-$ the strongest. That an acyl hydride is not observed in CH$_2$Cl$_2$ solution at all is consistent with rapid decarbonylation from the putative five-coordinate species in the absence of Lewis bases. The observation that **4** does not decarbonylate, while directly analogous **11** does, suggests that dissociation of the Rh−E bond (E = S or P), or steric constraints imposed by the PPh$_2$ group in the ring, are also important, as acetone dissociation would be expected to occur in both to form a vacant site. This further emphasizes that a balance must be struck between stabilization and reactivity in the onward hydroacylation reaction, as too strong a coordination will result in no reaction, albeit with no decarbonylation.[13]

Comments on the Overall Mechanism. Monitoring the catalytic hydroacylation of 1-octene with **2** using 10 mol % **1c** in d_6-acetone (0.075 M substrate) by NMR spectroscopy at 298 K showed the complete and pseudo-first-order formation of the linear ketone product with a rate constant of $(2.0 \pm 0.2) \times 10^{-3}$ s^{-1} ($t_{1/2} = 5.8 \pm 0.6$ min). Notably, this rate is considerably faster than decarbonylation of **11** in acetone at this temperature $(1.08 \pm 0.04) \times 10^{-4}$ s^{-1}. During and at the end of catalysis, the only observed species was the product-bound complex that arises from reductive coupling [Rh(^{t}Bu$_2$PCH$_2$P^{t}Bu$_2$)-{MeSC$_6$H$_4$CO(CH$_2$)$_7$Me}][BAr$^F_4$] (**18**), as indicated by NMR spectroscopy, ESI-MS, and independent synthesis from isolated product and **1c**. The decarbonylation product, **8**, was only observed in trace amounts by ESI-MS. Thus, under these conditions (10 mol % catalyst, acetone), productive catalysis clearly outruns decarbonylation. Repeating this catalytic experiment using 2-(methylthio)benzaldehdye-d_1 (d_1-**2**) resulted in slower overall catalysis. A H/D kinetic isotope effect (KIE) value of 1.5 ± 0.3 was measured. Similarly, a KIE value of 1.3 ± 0.3 was obtained from an initial rate study using 1 mol % **1c** in acetone (0.075 M substrate) at 328 K, where conversions were determined using HPLC (see Supporting Information). Moreover, inspection of the ^{1}H and ^{2}H NMR spectra of the final product obtained from catalysis using d_1-**2** show that deuterium is incorporated into methylene positions both α and β to the ketone carbonyl (Scheme 11), at δ 2.95 and 1.72, respectively, in a 1:4 ratio. That only the linear isomer of the ketone is observed as the final product to the detection limits of HPLC (i.e., a ratio of greater than 20:1 linear to branched)

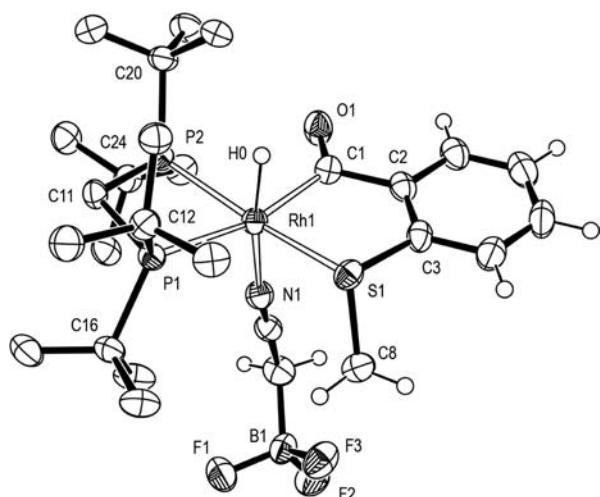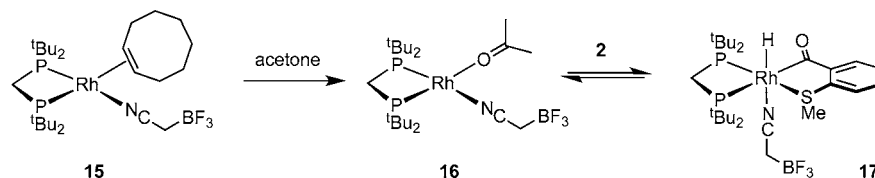**Scheme 9. Synthesis of [NCCH$_2$BF$_3$]$^-$ Ligated Complexes**
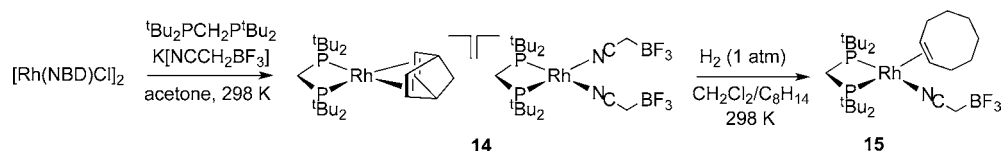
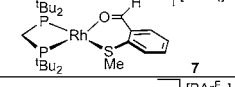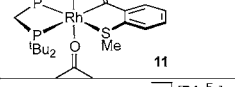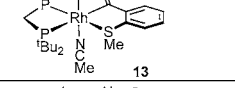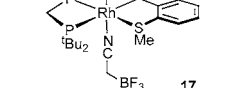**Scheme 10. Reactivity of [NCCH₂BF₃]⁻ Ligated Complexes with 2**
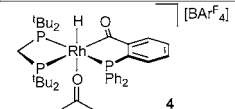
Figure 5. Solid-state structure of **17**; displacement ellipsoids depicted at the 50% probability level. Most hydrogen atoms and solvent molecules are omitted for clarity. Key bond lengths (Å) and angles (deg): Rh1−P1, 2.4626(11); Rh1−P2, 2.3264(10); Rh1−C1, 2.031(4); Rh1−S1, 2.3354(11); Rh1−H0, 1.61(4); Rh1−N1, 2.141(4); P1−Rh1−P2, 73.92(4); P1−C11−P2, 101.03(19); P1−Rh1−C1, 165.33(12); P2−Rh1−C1, 97.69(12); C1−Rh1−S1, 85.84(12); P1−Rh1−S1, 99.92(4); P2−Rh1−S1, 167.37(4); H0−Rh1−N1, 170.1(14); Lsq plane (Rh1, P1, P2, S1, C1), rms deviation = 0.097.

indicates that insertion of the hydride (deuteride) into the alkene is reversible and is occurring to give both linear and branched alkyl intermediates (intermediates **C** and **B** Scheme 11), but reductive elimination for the linear isomer has a considerably lower barrier.[8] ESI-MS demonstrates that there is a small amount of the d_0-product that could arise from β-elimination of a hydride to give **A** followed by alkene exchange.[65] Reversible hydride insertion has been noted previously.[6,8] Although linear selectivity is by far the most common in intermolecular hydroacylation systems using [Rh(diphosphine)]⁺ catalysts,[4] we have recently noted that sterically bulky ortho-substituted dppe-derived phosphines can direct excellent branched selectivity in alkyne hydroacylation.[14]

Rate-limiting reductive elimination of the final product would be expected to result in a negligible KIE, as no C−H bonds are being made or broken. Dong has recently reported a KIE of 1.79 ± 0.06 for intramolecular *aldehyde* hydroacylation, and when coupled with a Hammett study, suggested that this is due to the hydride insertion step being rate-limiting, rather than reductive elimination.[12] The oxidative addition of aldehydes on closely related cationic [Rh(dppp)]⁺ systems has been shown to have a KIE of 1.73 for phenylacetaldehyde, where migratory extrusion of CO is rate-determining,[66] while van Leeuwen and co-workers have shown that a small KIE of 1.22 ± 0.11 relates to the hydride migration step in the hydroformylation of 1-octene using Rh-Xantphos complexes, although they also note that CO dissociation and alkene coordination also contribute to the overall barrier.[67] Interestingly, a recent report by Hofmann and co-workers shows that for neutral Rh(ᵗBu₂PCH₂PᵗBu₂)-(Np)(η²-H₂C=CH₂) (Np = neopentyl) the barrier to alkyl migration is also high, such that this complex can be isolated and characterized in the solid-state (albeit at low temperature).[68]

Table 2. Relative Rates for the Formation of 8 from [Rh(ᵗBu₂PCH₂PᵗBu₂){SMe(C₆H₄CHO)}(L)]⁺ᵃ

Acyl Hydride	δ(hydride)	Solvent	Rate Constant / 10⁻⁶ s⁻¹	Half Life / hrs
4	−19.4	d₆-acetone	stable	
7	–	CD₂Cl₂	175 ± 3	1.10 ± 0.02
11	−20.3	d₆-acetone	108 ± 4	1.79 ± 0.06
13	−15.6	d₆-acetone	5.1 ± 0.3	38 ± 2
17	−15.5	d₆-acetone	2.7 ± 0.3ᵇ	73 ± 9ᵇ

ᵃRates reported for the first-order formation of **8**. ᵇOther products in addition to **8** are formed. The rate of acyl hydride decomposition is reported instead.

Scheme 11. Suggested Catalytic Cycle for the Hydroacylation of Alkenes with 2
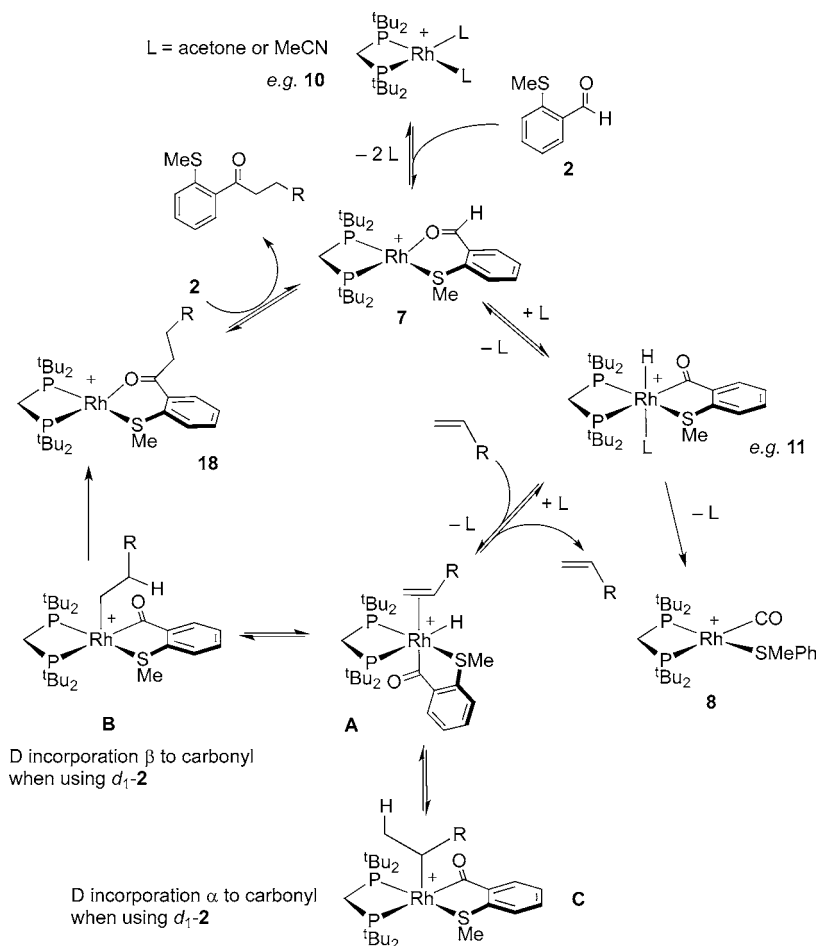
In our system, given the equilibria observed in both the stoichiometric studies and by deuterium labeling in catalysis, an "equilibrium isotope effect"[69] may also be operating. This means that the measurement of a small KIE ~ 1.4 in our system points only to irreversible oxidative addition not being a rate-limiting step, as this would be expected to result in a significant KIE. Scheme 11 summarizes our mechanistic interpretations.

Effect of Solvent and Concentration. Having established the overall rapid turnover of these small-bite-angle catalysts, that acyl hydrides are intermediates, and that decarbonylation follows a first-order process and can be attenuated to differing degrees by various Lewis bases, we next looked to bring these observations together to optimize the conditions for the intermolecular hydroacylation reaction. For this we used the reaction between aldehyde **2** and 1-octene. Table 3 outlines these studies.

At 10 mol % and 0.075 M aldehyde concentration (e.g., Figure 2), catalyst **1c** performed very well in dichloroethane solvent, outperforming the DPEphos catalyst **3** (entries 1 and 2). Reducing the catalyst loading to 1 mol % resulted in a significant drop in conversion, presumably as a consequence of decarbonylation (entry 4, Figure 6). ESI-MS of the postcatalyst solution confirmed this, with all the major peaks observed being attributed to carbonyl containing species, including **8** (see Supporting Information). Addition of more substrate to the postcatalysis solution resulted only in a small additional conversion (~10%) in the first hour and then no more.

Addition of small quantities of MeCN (ca. 2 equiv, entry 5) improved slightly the overall conversion using **1c**, as anticipated from the stoichiometric decarbonylation studies. However, catalysis in the presence of excess MeCN (greater than 2 equiv) attenuated catalysis (entries 6 and 7), presumably as the added MeCN increasingly outcompetes alkene coordination. Similarly, employing **15**, containing the strong binding anionic nitrile ligand, resulted in reduced conversion compared to **1c**. Using the preformed bis-acetonitrile complex **12c** (entry 8) gave the best improvement in comparison to **1c**. It is interesting to note that, in related zwitterionic Rh(I)−ligand complexes, *intramolecular* hydroacylation reactions can be run in neat MeCN.[21]

Changing solvent from dichloroethane to acetone demonstrated the stabilizing effect of the latter. Using both **1c** and **12c**, high conversions were achieved (e.g., entries 11 versus 3; Figure 7), with **12c** again giving the best results. Conversion using the DPEphos catalyst was also improved, but was still low (12 %). The effect of solvent (ClCH$_2$CH$_2$Cl versus acetone) is greater than that of added MeCN (entries 4/11 and 4/8, respectively; Figures 6 and 7), although both the effects are additive (entry 12). In addition to stabilization against decarbonylation, a recent computational analysis for the intramolecular hydroacylation of 4-pentenals using Rh(I)-dppe catalysts has suggested that Lewis bases (i.e., acetone/MeCN in our systems) can also play a role in reducing the barrier to reductive elimination.[11] Whatever the subtleties of the actual mechanism are here, our data show that the complex

Table 3. Catalyst Optimization[a]

Entry	Catalyst	Loading / mol%	Concentration / M	Solvent	Conversion / %
1	**3**	10	0.075	ClCH$_2$CH$_2$Cl	24
2	**1c**	10	0.075	ClCH$_2$CH$_2$Cl	96
3	**3**	1	0.075	ClCH$_2$CH$_2$Cl	4
4	**1c**	1	0.075	ClCH$_2$CH$_2$Cl	46
5	**1c** + 2 MeCN	1	0.075	ClCH$_2$CH$_2$Cl	50
6	**1c** + 10 MeCN	1	0.075	ClCH$_2$CH$_2$Cl	42
7	**1c** + 50 MeCN	1	0.075	ClCH$_2$CH$_2$Cl	32
8	**12c**	1	0.075	ClCH$_2$CH$_2$Cl	58
9	**15**	1	0.075	ClCH$_2$CH$_2$Cl	30
10	**3**	1	0.075	Acetone	12
11	**1c**	1	0.075	Acetone	80
12	**12c**	1	0.075	Acetone	91
13	**15**	1	0.075	Acetone	59
14	**3**	1	0.5	Acetone	48
15	**1c**	1	0.5	Acetone	94
16	**12c**	1	0.5	Acetone	99
17	**3**	0.1	0.5	Acetone	10
18	**1c**	0.1	0.5	Acetone	36
19	**12c**	0.1	0.5	Acetone	60
20	**3**	0.1	2.0	Acetone	39
21	**1c**	0.1	2.0	Acetone	100
22	**12c**	0.1	2.0	Acetone	100
23	**12c**	0.02	2.0	Acetone	17

[a]Conditions: ClCH$_2$CH$_2$Cl solvent, 353 K; acetone solvent, 328 K. Aldehyde (1.0 equiv) and alkene (1.5 equiv). Concentration refers to the concentration of aldehyde **2**. Conversions and selectivity are by HPLC. Linear isomer found in a greater than 20:1 ratio compared to the branched.
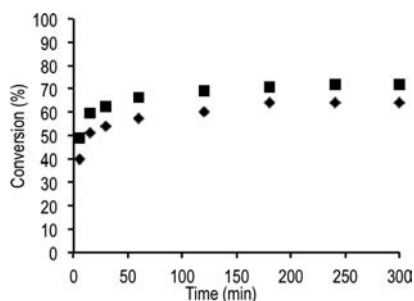

Figure 6. Time course plot for the hydroacylation of 1-octene (1.5 equiv) with **2** (1.0 equiv, 0.075 M) catalyzed by **1c** (◆) or **12c** (■). Conditions: 1 mol % catalyst, ClCH$_2$CH$_2$Cl, 353 K.[70]

Figure 7. Time course plot for the hydroacylation of 1-octene (1.5 equiv) with **2** (1.0 equiv, 0.075 M) catalyzed by **1c** (◆) or **12c** (■). Conditions: 1 mol % catalyst, acetone, 328 K.

using the preformed MeCN complex **12c** in acetone solvent results in the best catalyst at 1 mol % loadings.

In an effort to improve the performance of our catalysts further, we recognized that, as we had found decarbonylation to be independent of substrate concentration whereas for productive catalysis this was unlikely to be the case, increasing the overall substrate concentration could kinetically favor productive catalysis over decarbonylation. Pleasingly, this was the case, and entry 16 shows that at 1 mol % loading and 0.5 M aldehyde concentration essentially quantitative conversion was achieved using catalyst **12c**. **1c** also worked well (entry 15). Encouraged by these results, we looked to push the loadings to even lower levels of 0.1 mol %, which represent 2 orders of magnitude lower loadings than usually employed in these

reactions (*ca.* 10 mol %). Entry 19 shows that for **12c** 60% conversion could be achieved at 0.5 M aldehyde and 0.1 mol %. Using even more concentrated solutions (2.0 M aldehyde) improved this further and resulted in *quantitative conversion at 0.1 mol % loading* using either **1c** or **12c** as catalyst precursors (entry 21 and 22). These conversions correspond to turnover frequencies of *at least* 300 h^{-1} (unoptimized). The limit of the system was reached at 0.02 mol % (entry 23) with regard to a practicable and productive catalyst.

Demonstration of Reaction Scope. With effective catalysts in hand that operate at low loadings, we explored the scope of their application in intermolecular hydroacylation reactions, especially with substrates that have previously proved difficult to employ (Table 4). We have used both

Table 4. Scope of Alkene and Alkyne Hydroacylation Using 12a and 12c[a]

Entry	Aldehyde	Alkene/Alkyne	Catalyst (loading)	Product	Yield[b]
1			12c (0.1 mol%)		98%
2			12c (0.1 mol%)		78%
3			12c (0.1 mol%)		82%[c]
4			12c (0.1 mol%)		98%
5			12c (0.2 mol%)		95%
6			12a (5.0 mol%)		68%
7			12a (3.0 mol%)		81%
8			12a (2.0 mol%)		77%
9			12a (1.0 mol%)		75%[d]
10			12c (0.2 mol%)		84%
11			12c (0.2 mol%)		99%
12			12a (1.0 mol%)		83%
13			12c (0.1 mol%)		89%
14			12c (0.5 mol%)		92%
15			12a (1.0 mol%)		92%
16			12a (2.0 mol%)		87%

[a]Conditions: Aldehyde (1.0 equiv, 2.0 M), alkene, or alkyne (1.5 equiv), catalyst, acetone, 328 K, 3 h. [b]Linear isomers isolated with >20:1 selectivity (HPLC) in all cases, accept where stated otherwise. [c]Reaction performed at 353 K in ClCH$_2$CH$_2$Cl. [d]1.1:1 mixture of branched and linear isomers.

^{t}Bu$_2$PCH$_2$P^{t}Bu$_2$ (**12c**) and Cy$_2$PCH$_2$PCy$_2$ (**12a**) based bis-acetonitrile complexes to do this.

Using aldehyde **2**, the hydroacylation of several unactivated terminal alkenes was achieved using catalyst **12c** at 0.1–0.2 mol % loadings (entries 1–5). An interesting solvent effect was observed when the hydroacylation of 3-buten-1-ol was performed in DCE (entry 3), resulting in a cyclization/dehydration sequence to give the dihydropyran product. Importantly, employing these new catalysts has allowed the hydroacylation of more challenging substrates to be achieved. Disubstituted alkenes are significantly less reactive substrates in hydroacylation reactions; using DPEphos-catalyst **3** at 10 mol %, the hydroacylation of methyl methacrylate shows no detectable product after 18 h. However, using catalyst **12a**, both 1,1-disubstituted

and 1,2-disubstituted alkenes (entries 6 and 7) could be readily incorporated in 3 h. The hydroacylation of allenes provides easy access to β,γ-unsaturated ketones;[71] cyclohexylallene was hydroacylated with aldehyde **2** using 2 mol % of catalyst **12a** (entry 8). Butyl vinyl ether could also be hydroacylated using 1 mol % of **12a** to give a mixture of branched and linear isomers (entry 9). To our knowledge, this is the first example of the intermolecular hydroacylation of an enol ether.[72] These reactions clearly demonstrate the broad scope of alkene, alkyne, and allene substrates offered by these catalysts.

The aldehyde substrate could also be varied. Both electron rich (entry 10) and electron poor (entry 11) aryl aldehydes were incorporated with only 0.2 mol % of catalyst **12c**. A cyclohexene aldehyde (entries 12 and 13) underwent efficient hydroacylation of both alkyne and alkene substrates. Aliphatic aldehydes were also useful substrates, and they proceeded well in the hydroacylation of an alkene (entry 14) with 0.5 mol % of **12c** and an alkyne (entry 15) with 1% of **12a**. Finally, MTM-protected hydroxyacetaldehyde (entry 16) underwent alkyne hydroacylation with 2 mol % of **12a**. We have recently demonstrated the synthetic utility of the MTM protecting group as a removable directing group for hydroacylation, although catalyst loadings of 10 mol % have previously been required.[33]

CONCLUSIONS

We have outlined the development of new intermolecular hydroacylation catalysts based upon small-bite-angle ligands which allow for the union of β-S-substituted aldehydes with a wide variety of unactivated alkenes and alkynes. Through judicious choice of solvent and catalyst/substrate concentration, the unwanted decarbonylation deactivation pathway is attenuated while the productive hydroacylation reaction is enhanced to such an extent that very low catalyst loadings (0.1 mol %) and turnover frequencies of greater than 300 h^{-1} can be achieved. As these precatalyst systems are also readily prepared and bench-stable, they offer a practical solution for carrying out intermolecular hydroacylation reactions with β-tethered aldehydes. The high activity of these catalysts has also allowed previously challenging substrate classes to be included. Interestingly, high enantioselectives have previously been reported in Rh-mediated hydrogenations using asymmetric ligands closely related to $^{t}Bu_2PCH_2P^{t}Bu_2$,[73] and this encourages further development given the low loading and high-turnovers we report. With such efficient catalysts in hand the next challenge is to develop systems that do not require a β-tethered aldehyde.

ASSOCIATED CONTENT

Ⓢ Supporting Information
Full synthetic, crystallographic, and characterization details. This material is available free of charge via the Internet at http://pubs.acs.org. Crystallographic data have been deposited with the Cambridge Crystallographic Data Centre under CCDC Nos. 857099−857104. These data can be obtained free of charge from The Cambridge Crystallographic Data Centre via www.ccdc.cam.ac.uk/data_request/cif.

AUTHOR INFORMATION

Corresponding Author
andrew.weller@chem.ox.ac.uk; michael.willis@chem.ox.ac.uk

Notes
The authors declare no competing financial interest.

REFERENCES

(1) Suggs, J. W. *J. Am. Chem. Soc.* **1978**, *100*, 640.
(2) Sakai, K.; Ide, J.; Oda, O.; Nakamura, N. *Tetrahedron Lett.* **1972**, *13*, 1287.
(3) Lochow, C. F.; Miller, R. G. *J. Am. Chem. Soc.* **1976**, *98*, 1281.
(4) Willis, M. C. *Chem. Rev.* **2009**, *2010*, 725.
(5) Fairlie, D. P.; Bosnich, B. *Organometallics* **1988**, *7*, 936.
(6) Fairlie, D. P.; Bosnich, B. *Organometallics* **1988**, *7*, 946.
(7) Lenges, C. P.; Brookhart, M. *J. Am. Chem. Soc.* **1997**, *119*, 3165.
(8) Roy, A. H.; Lenges, C. P.; Brookhart, M. *J. Am. Chem. Soc.* **2007**, *129*, 2082.
(9) Bosnich, B. *Acc. Chem. Res.* **1998**, *31*, 667.
(10) Moxham, G. L.; Randell-Sly, H.; Brayshaw, S. K.; Weller, A. S.; Willis, M. C. *Chem.—Eur. J.* **2008**, *14*, 8383.
(11) Hyatt, I. F. D.; Anderson, H. K.; Morehead, A. T.; Sargent, A. L. *Organometallics* **2008**, *27*, 135.
(12) Shen, Z.; Dornan, P. K.; Khan, H. A.; Woo, T. K.; Dong, V. M. *J. Am. Chem. Soc.* **2009**, *131*, 1077.
(13) Pawley, R. J.; Moxham, G. L.; Dallanegra, R.; Chaplin, A. B.; Brayshaw, S. K.; Weller, A. S.; Willis, M. C. *Organometallics* **2010**, *29*, 1717.
(14) González-Rodríguez, C.; Pawley, R. J.; Chaplin, A. B.; Thompson, A. L.; Weller, A. S.; Willis, M. C. *Angew. Chem., Int. Ed.* **2011**, *50*, 5134.
(15) Bergens, S. H.; Fairlie, D. P.; Bosnich, B. *Organometallics* **2002**, *9*, 566.
(16) Fuji, K.; Morimoto, T.; Tsutsumi, K.; Kakiuchi, K. *Chem. Commun.* **2005**, 3295.
(17) Khan, H. A.; Kou, K. G. M.; Dong, V. M. *Chem. Sci.* **2011**, *2*, 407.
(18) Shibahara, F.; Bower, J. F.; Krische, M. J. *J. Am. Chem. Soc.* **2008**, *130*, 14120.
(19) Omura, S.; Fukuyama, T.; Horiguchi, J.; Murakami, Y.; Ryu, I. *J. Am. Chem. Soc.* **2008**, *130*, 14094.
(20) Goikhman, R.; Milstein, D. *Angew. Chem., Int. Ed.* **2001**, *40*, 1119.
(21) Betley, T. A.; Peters, J. C. *Angew. Chem., Int. Ed.* **2003**, *42*, 2385.
(22) Hoffman, T. J.; Carreira, E. M. *Angew. Chem., Int. Ed.* **2011**, *50*, 10670.
(23) Jun, C. H.; Jo, E. A.; Park, J. W. *Eur. J. Org. Chem.* **2007**, 1869.
(24) Tanaka, K.; Shibata, Y.; Suda, T.; Hagiwara, Y.; Hirano, M. *Org. Lett.* **2007**, *9*, 1215.
(25) Kokubo, K.; Matsumasa, K.; Nishinaka, Y.; Miura, M.; Nomura, M. *Bull. Chem. Soc. Jpn.* **1999**, *72*, 303.
(26) Imai, M.; Tanaka, M.; Tanaka, K.; Yamamoto, Y.; Imai-Ogata, N.; Shimowatari, M.; Nagumo, S.; Kawahara, N.; Suemune, H. *J. Org. Chem.* **2004**, *69*, 1144.
(27) Coulter, M. M.; Kou, K. G. M.; Galligan, B.; Dong, V. M. *J. Am. Chem. Soc.* **2010**, *132*, 16330.
(28) Willis, M. C.; McNally, S. J.; Beswick, P. J. *Angew. Chem., Int. Ed.* **2004**, *43*, 340.
(29) Willis, M. C.; Randell-Sly, H. E.; Woodward, R. L.; Currie, G. S. *Org. Lett.* **2005**, *7*, 2249.
(30) Willis, M. C.; Randell-Sly, H. E.; Woodward, R. L.; McNally, S. J.; Currie, G. S. *J. Org. Chem.* **2006**, *71*, 5291.
(31) Osborne, J. D.; Randell-Sly, H. E.; Currie, G. S.; Cowley, A. R.; Willis, M. C. *J. Am. Chem. Soc.* **2008**, *130*, 17232.
(32) Osborne, J. D.; Willis, M. C. *Chem. Commun.* **2008**, 5025.
(33) Parsons, S. R.; Hooper, J. F.; Willis, M. C. *Org. Lett.* **2011**, *13*, 998.
(34) Lenden, P.; Ylioja, P. M.; Gonzalez-Rodriguez, C.; Entwistle, D. A.; Willis, M. C. *Green Chem.* **2011**, *13*, 1980.
(35) Moxham, G. L.; Randell-Sly, H. E.; Brayshaw, S. K.; Woodward, R. L.; Weller, A. S.; Willis, M. C. *Angew. Chem., Int. Ed.* **2006**, *45*, 7618.

4896

dx.doi.org/10.1021/ja211649a | *J. Am. Chem. Soc.* 2012, 134, 4885−4897

(36) Brookhart has reported a Co(I)-based system than can work at low (1%) loadings, but the alkene component is limited to vinyl silanes. See ref 7.

(37) Brown, J. M.; Guiry, P. J. *Inorg. Chim. Acta* **1994**, *220*, 249.

(38) Marcone, J. E.; Moloy, K. G. *J. Am. Chem. Soc.* **1998**, *120*, 8527.

(39) Freixa, Z.; van Leeuwen, P. W. N. M. *Dalton Trans.* **2003**, 1890.

(40) Leeuwan, P.; Chadwick, J. *Homogeneous Catalysts: Activity−Stability−Deactivation*; Wiley−VCH: Weinheim, 2011.

(41) Hofmann, P.; Meier, C.; Englert, U.; Schmidt, M. U. *Chem. Ber* **1992**, *125*, 353.

(42) Hofmann, P.; Meier, C.; Hiller, W.; Heckel, M.; Riede, J.; Schmidt, M. U. *J. Organomet. Chem.* **1995**, *490*, 51.

(43) Eisentrager, F.; Gothlich, A.; Gruber, I.; Heiss, H.; Kiener, C. A.; Kruger, C.; Ulrich Notheis, J.; Rominger, F.; Scherhag, G.; Schultz, M.; Straub, B. F.; Volland, M. A. O.; Hofmann, P. *New J. Chem.* **2003**, *27*, 540.

(44) Urtel, H.; Meier, C.; Eisentrager, F.; Rominger, F.; Joschek, J. P.; Hofmann, P. *Angew. Chem., Int. Ed.* **2001**, *40*, 781.

(45) Luedtke, A. T.; Goldberg, K. I. *Inorg. Chem.* **2007**, *46*, 8496.

(46) Lanci, M. P.; Remy, M. S.; Lao, D. B.; Sanford, M. S.; Mayer, J. M. *Organometallics* **2011**, *30*, 3704.

(47) Manger, M.; Wolf, J.; Teichert, M.; Stalke, D.; Werner, H. *Organometallics* **1998**, *17*, 3210.

(48) DuBois, D. L.; Blake, D. M.; Miedaner, A.; Curtis, C. J.; DuBois, M. R.; Franz, J. A.; Linehan, J. C. *Organometallics* **2006**, *25*, 4414.

(49) Wilson, A. D.; Miller, A. J. M.; DuBois, D. L.; Labinger, J. A.; Bercaw, J. E. *Inorg. Chem.* **2010**, *49*, 3918.

(50) Reid, S. M.; Mague, J. T.; Fink, M. J. *J. Am. Chem. Soc.* **2001**, *123*, 4081.

(51) Urtel, H.; Bikzhanova, G. A.; Grotjahn, D. B.; Hofmann, P. *Organometallics* **2001**, *20*, 3938.

(52) Wass, D. F. *Dalton Trans.* **2007**, 816.

(53) Theodor, A. *Coord. Chem. Rev.* **2011**, *255*, 861.

(54) Douglas, T. M.; Brayshaw, S. K.; Dallanegra, R.; Kociok-Kohn, G.; Macregor, S. A.; Moxham, G. L.; Weller, A. S.; Wondimagegn, T.; Vadivelu, F. *Chem.—Eur. J.* **2008**, *14*, 1004.

(55) Douglas, T. M.; Chaplin, A. B.; Weller, A. S. *Organometallics* **2008**, *27*, 2918.

(56) Dallanegra, R.; Robertson, A. P. M.; Chaplin, A. B.; Manners, I.; Weller, A. S. *Chem. Commun.* 2011, *47*, 3763.

(57) Ficker, R. Technische Universitat, Munchen, Germany. Structure deposited in the CCDC: CCDC 107454, 1995.

(58) Lee, H.; Jun, C. H. *Bull. Korean Chem. Soc.* **1995**, *16*, 66.

(59) Lee, H.; Jun, C. H. *Bull. Korean Chem. Soc.* **1995**, *16*, 1135.

(60) Albrecht, M. *Chem. Rev.* **2009**, *110*, 576.

(61) Adams, H.; Bailey, N. A.; Mann, B. E.; Manuel, C. P. *Inorg. Chim. Acta* **1992**, *198−200*, 111.

(62) Cooper, A. C.; Clot, E.; Huffman, J. C.; Streib, W. E.; Maseras, F.; Eisenstein, O.; Caulton, K. G. *J. Am. Chem. Soc.* **1999**, *121*, 97.

(63) Compound **5** can also be prepared by addition of (*o*-PPh₂)C₆H₄CHO to **12c**. See Supporting Information.

(64) Molander, G. A.; Ham, J. *Org. Lett.* **2006**, *8*, 2031.

(65) We cannot discount that this product also arises from trace 2 in the sample of *d₁*-**2**.

(66) Fristrup, P.; Kreis, M.; Palmelund, A.; Norrby, P.-O.; Madsen, R. *J. Am. Chem. Soc.* **2008**, *130*, 5206.

(67) Zuidema, E.; Escorihuela, L.; Eichelsheim, T.; Carbó, J. J.; Bo, C.; Kamer, P. C. J.; van Leeuwen, P. W. N. M. *Chem.—Eur. J.* **2008**, *14*, 1843.

(68) Urtel, H.; Meier, C.; Rominger, F.; Hofmann, P. *Organometallics* **2010**, *29*, 5496.

(69) Jones, W. D. *Acc. Chem. Res.* **2002**, *36*, 140.

(70) In our hands conversions in DCE solvent can vary by ±10%, while those in acetone are more consisent. This might point to reactivity between the catalyst and the solvent. See, for example: Vetter, A. J.; Rieth, R. D.; Brennessel, W. W.; Jones, W. D. *J. Am. Chem. Soc.* **2009**, *131*, 10742 and references therin.

(71) Randell-Sly, H. E.; Osborne, J. D.; Woodward, R. L.; Currie, G. S.; Willis, M. C. *Tetrahedron* **2009**, *65*, 5110.

(72) For an example of the intermolecular Rh-catalyzed hydroacylation of an enamide, see: Zhang, J.-J.; Bolm, C. *Org. Lett.* **2011**, *13*, 3900.

(73) Hoge, G.; Wu, H.-P.; Kissel, W. S.; Pflum, D. A.; Greene, D. J.; Bao, J. *J. Am. Chem. Soc.* **2004**, *126*, 5966.

4897

dx.doi.org/10.1021/ja211649a | *J. Am. Chem. Soc.* 2012, 134, 4885−4897